Flowing Fluid Electric Conductivity Logging for a Deep Artesian Well in Fractured Rock with Regional Flow

Christine Doughty[1], Chin-Fu Tsang[1, 2], Satoshi Yabuuchi[3] and Takanori Kunimaru[3]

[1]Earth Sciences Division
Lawrence Berkeley National Laboratory
Berkeley, CA, USA 94720

[2]Department of Earth Sciences, Uppsala University
Uppsala, SE-75236, Sweden

[3]Japan Atomic Energy Agency
Geological Isolation Research and Development Directorate
Horonobe Underground Research Center, Hokkaido, JAPAN

March 2012

Abstract

The flowing fluid electric conductivity (FFEC) logging method is a well-logging technique that may be used to estimate flow rate, salinity, transmissivity, and hydraulic head of individual fractures or high-permeability zones intersected by a wellbore. Wellbore fluid is first replaced with fluid of a contrasting electric conductivity, then repeated FEC logging is done while the well is pumped. Zones where fluid flows into the wellbore show peaks in the FEC logs, which may be analyzed to infer inflow rate and salinity of the individual fractures. Conducting the procedure with two or more pumping rates (multi-rate FFEC logging) enables individual fracture transmissivity and hydraulic head to be determined. Here we describe the first application of the multi-rate FFEC logging method to an artesian well, using a 500-m well in fractured rock at Horonobe, Japan. An additional new factor at the site is the presence of regional groundwater flow, which heretofore has only been studied with synthetic data. FFEC logging was conducted for two different pumping rates. Several analysis techniques had to be adapted to account for the artesian nature of the well. The results were subsequently compared with independent salinity measurements and transmissivity and hydraulic head values obtained from packer tests in the same well. Despite non-ideal operating conditions, multi-rate FFEC logging successfully determined flow rate, salinity, and transmissivity of 17 conducting fractures intercepted by the logged section of the borehole, including two fractures with regional groundwater flow. Predictions of hydraulic head were less accurate, a not unexpected result in light of operational problems and the form of the equation for hydraulic head, which involves the difference between two uncertain quantities. This study illustrates the strengths and weaknesses of the multi-rate FFEC logging method applied to artesian wells. In conjunction with previous studies, it demonstrates the usefulness of the method for a broad range of conditions encountered in subsurface fractured rock.

Keywords

Borehole logging; Fluid electric conductivity logging; Hydrogeologic characterization; Characterization of fractured rock; Identification of fracture flow

1. Introduction

Knowledge of the locations and hydraulic properties of conductive features is needed to understand flow and transport through fractured rocks, which is required for a variety of practical applications, including geologic storage of nuclear waste, toxic chemicals and carbon dioxide, and exploitation of natural resources such as petroleum and geothermal fluids. Boreholes drilled deep into the rock are often employed to obtain this information. Various downhole methods for studying fracture flow have been developed over the past few decades. Coring and borehole imaging methods (e.g. video camera, borehole televiewer) may be able to locate and categorize the fractures by type and orientation, but they are unlikely to provide direct information on fracture flow properties (Keys, 1979; Paillet, 1991; Bear et al., 1993). Straddle-packer pump-testing is a widely-used, well-accepted method for obtaining fracture flow properties (Almen, 1994; National Research Council, 1996; Enachescu and Rahm, 2007), and an advanced deployment known as hydraulic tomography, which uses a systematic choice of packed-off intervals, allows for the reconstruction of two- and three-dimensional images of the subsurface (Karasaki et al., 2000; Brauchler et al., 2003; Illman et al, 2009); these methods tend to be very time-consuming and thus expensive. Flow-logging techniques are an attractive alternative – they measure flow directly and are efficient to deploy in the field. Several varieties of flow logging exist, including spinner surveys (Molz et al., 1989), heat-pulse flowmeters (Öhberg and Rouhiainen, 2000; Paillet, 1998; Paillet and Pedler, 1996), tracer dilution analysis (Brainerd and Robbins, 2004), and the flowing fluid electric conductivity (FFEC) logging method, the technique employed in the present study.

FFEC logging is what is known as a hydrogeophysical method, in that it uses geophysical measurements to obtain hydrological information about the subsurface. Hydrogeophysics is a rapidly growing field (Rubin and Hubbard, 2005; Vereecken et al., 2006; Kowalsky et al., 2011) that makes use of the complementary aspects of geophysical and hydrological data to gain understanding of and reduce uncertainty about

complex, inherently unknowable subsurface hydrogeological systems, of which fractured rock is a prime example.

To initiate the FFEC logging method, wellbore fluid is replaced with water of constant salinity different from that of the formation water. FEC profiles in the wellbore are then measured at a series of times while the well is pumped at a constant rate. Locations where native fluid enters the wellbore show peaks in the FFEC logs. By fitting the growth and movement of these peaks with a simple numerical model, one can infer inflow strengths and salinities of individual permeable features intersected by the borehole. Since Tsang et al. (1990) introduced the method, it has been widely applied in deep wells down to 1500 m or more (Doughty et al., 2005, 2008; Guyonnet et al., 1993; Kelley et al., 1991; Löw et al., 1994), in inclined boreholes drilled in the underground Grimsel Test Laboratory (Marschall and Vomvoris, 1995), and extensively in shallower wells down to about 100 m (Bauer and LoCoco, 1996; Evans, 1995; Evans et al., 1992; Karasaki et al., 2000; Paillet and Pedler, 1996; Pedler et al., 1992). Continued development of analytical and numerical data-analysis techniques (e.g., Doughty and Tsang, 2005) has broadened the range of applicability and enhanced the ease of use of the method. In particular, repeated logging using several pumping rates, known as multi-rate FFEC logging (Tsang and Doughty, 2003), enables transmissivity and hydraulic head of individual permeable features to be determined. Note that FFEC logging requires little or no specialized equipment or expertise, and may be carried out more quickly than most other methods, making it a valuable tool for efficient subsurface characterization.

This paper presents the first application of the multi-rate FFEC logging method to an artesian well, using a 500-m well in fractured rock at Horonobe, Japan. The key difficulties associated with an artesian well are that it may be difficult or impossible to establish uniform initial conditions for FFEC logging, obtain a simple direct relationship between flow rate and drawdown, and, most importantly, maintain a constant flow rate out of the well during logging,. An additional special feature of this study is the identification of natural groundwater flow in several of the fractures, whose magnitude is estimated by the FFEC logging method. The next section gives a general description of

the FFEC logging analysis method. The field data are then presented, followed by the analysis of these data. The results of the analysis are then compared with those of packer tests conducted in the same borehole. The paper concludes with a discussion of issues encountered in logging an artesian well and their consequences for the applicability of FFEC logging.

2. Methodology

This section gives a general summary of data collection and analysis methods involved in the FFEC logging method. Further details of the data collection method may be found in Doughty et al. (2005) and further details of the analysis method may be found in Doughty and Tsang (2005), Doughty et al. (2005), Tsang and Doughty (2003), and Tsang et al. (1990).

2.1 Data Collection

In the FFEC logging method, the wellbore water is first replaced by water of a constant salinity different from that of the formation water. This may be accomplished by injecting de-ionized (DI) water through a tube to the bottom of the wellbore at a low rate, while simultaneously pumping from the top of the well at the same rate (recirculation phase). The goal is to completely replace the wellbore water with DI water without altering wellbore hydraulic head, so that no DI water is pushed out into the formation nor is any formation water pulled into the well. The FEC of the effluent is monitored throughout the recirculation period, which continues until a low stable FEC value is reached. If the final, stable, effluent FEC is substantially higher than the DI-water FEC, it indicates that native fluid is entering the wellbore during recirculation. This may occur because wellbore hydraulic head was unintentionally dropped during recirculation, or if natural groundwater flow is intercepted by the well. It can also occur if different permeable features intercepted by the wellbore have different hydraulic heads, which sets up an internal wellbore flow, with formation water entering the wellbore through features with higher hydraulic head and borehole water entering the formation through features with lower hydraulic head.

Next, the well is shut in (i.e., injection and pumping are stopped) and the DI water tube is removed. Then the well is pumped from the top at a constant low flow rate Q_1 (e.g., several or tens of liters per minute), while an electric conductivity probe is lowered into the wellbore to scan the FEC as a function of depth. This produces what is known as a flowing FEC (or FFEC) log or profile. With constant pumping conditions, a series of five or six FFEC logs are typically obtained over a one- or two-day period. Throughout the process, the water level in the well is monitored. Optionally, the entire procedure may be repeated using a different pumping rate Q_2, typically half or double the original rate Q_1. A useful option is to conduct the logging once more with $Q = 0$, which has the advantage of investigating natural groundwater flow and internal wellbore flow directly. For an artesian well, it may not be practical to log with $Q = 0$, but it is possible to use the natural flow of the well for Q_1, as long as flow rate is measured to assure that it remains constant during logging.

2.2 Data Analysis

Data analysis techniques include three main methods: 1) direct fitting of the time-series of FFEC profiles with a numerical model (Tsang et al., 1990), which yields the locations, inflow strengths, and salinities of permeable features: 2) the mass-integral method (Doughty and Tsang, 2005), in which each FFEC profile is integrated over the entire logged interval to provide an estimate of salt mass in place as a function of time, which can provide useful constraints on the direct fitting process; 3) multi-rate FFEC analysis (Tsang and Doughty, 2003), which enables the transmissivities and hydraulic heads of the different permeable features to be determined.

The numerical models BORE (Hale and Tsang, 1988) and the enhanced version BORE II (Doughty and Tsang, 2000) are used for direct fitting of the FFEC logs; they calculate the time evolution of ion concentration (salinity) in the wellbore during FFEC logging by solving the one-dimensional advection-dispersion equation, given a pumping rate Q and a set of feed-point locations z_i, strengths q_i, and salinities C_i (i.e., the forward problem). Fluid flow in the wellbore is considered to be quasi-steady: that is, fluid is

assumed to be incompressible so it responds instantly to changes in pumping rate or feed-point strength. Under typical FFEC logging conditions, pumping rate is kept fixed (or nearly fixed) for hours at a time, and the FFEC profiles measured reflect an integration of flow conditions over one or more hours, justifying the incompressibility assumption. Density differences between the original wellbore fluid (DI or low-salinity water, which may contain traces of drilling mud) and formation fluid flowing into the wellbore are neglected. If natural groundwater flow or internal wellbore flow occurs during recirculation, then a non-uniform salinity profile develops along the borehole before logging begins, which may be accounted for by specifying a non-uniform salinity profile $C_0(z)$ as the initial condition for the model. The governing equations for BORE II are presented in Doughty and Tsang (2005).

The general procedure for using BORE II for direct fitting is to assign feed-point locations z_i by identifying individual peaks in the early-time FFEC profiles, then to assign feed-point properties (q_i and C_i) by trial and error until an acceptable match between modeled and observed FFEC profiles is obtained (i.e., an inverse problem). In multi-rate FFEC analysis, the inverse procedure is repeated for each value of Q, with the inverse problems constrained by requiring that the same set of z_i and C_i values be used for each one. Assuming that two sets of FFEC logs were collected with pumping rates Q_1 and Q_2, and that the strengths of individual feed points i, as evaluated by BORE II, are $q_i^{(1)}$ and $q_i^{(2)}$ respectively, then Tsang and Doughty (2003) and Doughty and Tsang (2005) showed that the normalized transmissivity for each feed point is

$$\frac{T_i}{T_{tot}} = \frac{q_i^{(1)} - q_i^{(2)}}{Q_1 - Q_2}, \tag{1}$$

and the normalized hydraulic head for each feed point is

$$I\Delta P_i = \left(\frac{q_i^{(1)} / Q_1}{T_i / T_{tot}} - 1 \right) Q_1, \tag{2}$$

where T_i/T_{tot} is the fraction of the total transmissivity of the logged interval corresponding to the fracture or permeable zone represented by the ith feed point ($\Sigma T_i/T_{tot} = 1$) and $\Delta P_i = P_i - P_{avg}$ where P_i is the inherent hydraulic head of fracture i and P_{avg} is the stabilized hydraulic head in the wellbore when it is shut in for an extended time. I is a ratio known

as the productivity index (in the petroleum literature) or specific capacity (in hydrology), which is defined as the ratio of pumping rate to steady-state drawdown during a well test. I characterizes the entire permeable formation intersected by the wellbore in an average sense under steady-state flow conditions. In the FFEC context, I is approximated as

$$I = \frac{Q_1}{P_{avg} - P_{wb}^{(1)}} \tag{3}$$

where $P_{wb}^{(1)}$ is the hydraulic head in the wellbore (presumed constant) during the FFEC logging at $Q = Q_1$.

The derivation of Equations (1) and (2) assumes that the flow geometries within all the hydraulically conductive fractures intersecting the borehole are the same (e.g., all radial flow or all linear flow). The inherent (also known as far-field) hydraulic head P_i is the ambient or undisturbed hydraulic head in a fracture (or permeable layer), and it is the value that would be measured under non-pumping conditions with inflated packers in the wellbore on either side of the fracture to isolate it for a substantial time period to attain steady-state pressure conditions. In contrast, P_{avg} is the value that would be measured under non-pumping, shut-in conditions with the wellbore open to all feed points in the logged interval for a substantial time period (for an artesian well, shut in means the well is capped to prohibit natural flow at the surface). P_{avg} can be calculated as a transmissivity-weighted average over all P_i values: $P_{avg} = \Sigma(T_i P_i)/T_{tot}$. The hydraulic head difference $\Delta P_i = P_i - P_{avg}$ provides a measure of the driving force for fluid flow between hydraulically conducting fractures and the wellbore under shut-in conditions, which gives rise to internal wellbore flow. Note that from the definition of P_{avg} above, if all the P_i values are the same, then $P_i = P_{avg}$, so that all $\Delta P_i = 0$, and there will be no internal wellbore flow under shut-in conditions. In this case, Equation (2) shows that feed-point strength q_i is proportional to fracture transmissivity T_i, making it possible to determine T_i/T_{tot} by matching FFEC profiles for just one pumping rate Q.

3. Field Data

The artesian well used for the present study, known as PB-V01, is located in Horonobe town, in the northernmost part of Hokkaido, Japan, where hydrogeochemical investigations are being conducted under the auspices of the Japan Atomic Energy Agency (JAEA) to develop technologies and methodologies that may in future be applied to sites being considered for geological disposal of high-level radioactive waste in sedimentary rock in Japan. Horonobe overlies Neogene sedimentary sequences (in ascending order: Souya coal-bearing Formation, Masuhoro Formation, Wakkanai Formation, Koetoi Formation, and Yuchi Formation), which are underlain by an igneous and Palaeogene-to-Cretaceous sedimentary basement. Borehole PB-V01 intercepts the Wakkanai and Koetoi Formations, which are composed of Neogene argillaceous sedimentary rocks that have low intrinsic permeability but are highly fractured (Hama et al., 2007; Doughty et al., 2008).

3.1 Borehole Geometry and Log Data

The interval of borehole PB-V01 being investigated by the FFEC logging method is between 131 and 506 m below the ground surface. The well ends just below the bottom of the logged interval. There is no packer at the top of logged interval and the well is cased above the logged interval. The wellbore diameter near the surface (where the water level changes during logging) is 22 cm. The caliper log (Figure 1) indicates that the uncased borehole diameter is somewhat variable, ranging from 16 cm at the deepest part of the logged interval to 18 cm at the shallowest part. Over most of the logged interval, the depth-averaged diameter used in the BORE II model, 16.6 cm, is a good representation of the actual wellbore diameter. The smaller diameter at depths below 470 m means that actual peaks will move upward slightly more quickly than modeled peaks there, and the larger diameter at depths above 190 m means that actual peaks will move upward slightly more slowly than modeled peaks there.

Feed-point depths inferred from visual examination of early-time peaks in FFEC logs are also shown in Figure 1, along with a fracture log obtained from core analysis. Comparison of these two quantities indicates that feed points (flowing fractures) form a

small subset of all observed fractures This is typical of fractured rock and, in general, it is well known that among the fractures found in a fracture log, only about 10% have significant hydraulic conductivity (Rhen and Hartley, 2009). This emphasizes the need for direct hydraulic characterization methods, such as FFEC logging, flow meters, packer tests, or tracer tests, that examine the flow properties of the fractures, not merely their existence.

3.2 Pumping Rate and Water-Level Data

The pumping rate was highly variable during FFEC logging (Figure 2). The artesian nature of borehole PB-V01 makes controlling pumping rate difficult. For Test 1, the nominal pumping rate was 8 L/min, but the actual pumping rate ranged from about 2 L/min to 10 L/min, with a time-averaged value of 6.7 L/min. For Test 2, the nominal pumping rate was 16 L/min, but the actual pumping rate ranged from 12 L/min to 20 L/min, with a time-averaged value of 14.3 L/min. The initial analyses of both tests used a single time-averaged pumping rate, shown as a black dashed line in Figure 2. For Test 2, the final two FFEC profiles were not used in the match. After the multi-rate analysis was completed, which provides a prescription for how individual feed-point strengths should change when pumping rate changes, Test 2 was modeled with a two-step pumping rate, as shown by the red dashed line in Figure 2.

The water-level data is shown in Figure 3. Note that the total drawdown for Test 1 is about 6 m, whereas that for Test 2 is about 24 m, a factor of four greater, although the pumping rate is roughly doubled from Test 1 to Test 2. This finding is consistent with the notion that the well is artesian – some flow occurs with no drawdown at all. An added complication is that within each test, variations in pumping rate (Figure 2) do not always produce the expected response in water level (Figure 3). For example, 4 hours into Test 2, pumping rate decreased significantly, and shortly thereafter water level also decreased sharply.

When the water level in a well is changing during logging, the pumping rate Q is assumed to be the sum of two parts: water coming out of the formation, Q_{form}, and water

coming out of the wellbore, Q_{well}, which is calculated as the product of water-level decline rate and wellbore cross-sectional area. A rough estimate of Q_{well} is 0.6 L/min for Test 1 (6 m drawdown in 6 hours and a cross-sectional area of $A = \pi(0.22/2)^2 = 0.038$ m^2) and 2.5 L/min for Test 2 (24 m drawdown in 6 hours). Applying this correction to the time-averaged pumping rates yields Q_{form} = 6.1 L/min for Test 1 and Q_{form} = 11.8 L/min for Test 2.

During artesian logging, the flow rate out of the top of the borehole was not recorded, but the water-level decline is assumed to be zero (artesian conditions) so that $Q = Q_{form}$.

3.3 FFEC Data

Recirculation of low-FEC water (10-13 mS/m) was done at a high pumping rate, 150 L/min for Test 1 and 100 L/min for Test 2, under overflow conditions. Recirculation continued until the effluent FEC values had stabilized at about 50-65 mS/m. Several hours after recirculation ended, an FFEC profile was collected without pumping the well, a procedure referred to as artesian logging. One and one-half hours thereafter, the main FFEC logging commenced, with the well pumped at an average rate of 6.7 L/min for Test 1 and 14.3 L/min for Test 2, with a total of six logs collected for each test. Each log took about 25 minutes to collect (the probe moves 15 m/min and the logging interval is 380 m long). Figure 4 and Figure 5 show the FFEC logs for Test 1 and Test 2, respectively. The profiles are color coded to match the boxes shown in Figures 2 and 3.
FEC data is temperature dependent, and the temperature along the logged interval is also collected so that FEC data can be corrected to a temperature of 20^{o}C, using a correlation developed from Schlumberger (1984): $FEC(20^oC) = FEC(T)/[1 + S(T - 20^oC)]$, with $S = 0.024^oC^{-1}$. All FFEC profiles shown here have been temperature-corrected.

Figure 4 shows that for Test 1, peaks grow monotonically, which is consistent with our conceptual model that time-variations of feed-point strength resulting from time-variation of pumping rate are small enough to be neglected, and moreover that the salinity for each feed point does not change with time. In contrast, Figure 5 shows that for Test 2, peaks grow monotonically only for the first two hours, then show a decline

between the second and fourth hours, then again grow between the fourth and fifth hour. Such a variation cannot be explained within our conceptual model. Even if the decrease in total-well pumping rate at t = 4 hours is included, which would cause a decrease in feed-point strength, it cannot explain a peak decrease between t = 2 hours and t = 3 hours. Therefore, only the first three profiles are used for the matching process. The unexplained peak decrease could be the result of a malfunction of the FEC probe or some aspect of the data collection system (note that the noise in the FFEC profiles seems to be larger for higher FEC values). Alternatively, the salinity of the water flowing from the fractures could be decreasing with time, resulting in a lowering of peaks. Time-varying salinity within a given fracture is certainly possible, given the potential for variability of salinity between fractures and the likely interconnectedness of the fractures intersecting the wellbore. However, the manner in which salinity decreases – concurrently at the largest peaks – argues in favor of instrument error.

Figure 6 shows the FFEC profiles collected during artesian logging (logging when the well is not actively pumped). These profiles were collected 2.75 hours after recirculation ended for Test 1, and 2 hours after recirculation ended for Test 2. It is not known at what rate fluid was flowing out of the top of the well while these logs were collected, but it is clear from the skewed nature of the peaks that fluid is flowing upward through the wellbore in the logged interval. The $t = 0$ profiles for Test 1 and Test 2 were collected when active pumping began for each test. For both tests, a period of 1.5 hours elapsed between the artesian logging and the beginning of the test. Comparing the $t = 0$ profiles in Figure 4 and Figure 5 with the artesian profiles in Figure 6 indicates that further skewing of the peaks occurred during this time, suggesting continued upflow.

4. Analysis

4.1 Approach

The first step in the BORE II analysis is to determine feed-point depths z_i by eye from the FFEC profiles shown in Figures 4, 5, and 6. Early-time profiles, before the peaks

from each feed point have begun to interfere with each other are most useful for this purpose. The feed-point depths can be determined quite accurately and are shown on Figure 1. Note that we do not use the fracture log shown in Figure 1 to infer feed-point location.

Next, the FFEC profiles for Test 1 are fit by modeling Test 1 as having a constant pumping rate, and adjusting feed-point strength q_i and salinity C_i (in terms of fluid electric conductivity) by trial and error. An estimate of the dispersion coefficient, which controls how much mixing occurs within the wellbore, thus spreading out the peaks, is also needed. The $t = 0$ profile is used as the initial condition for the model.

Then, the first three FFEC profiles of Test 2 are fit by modeling Test 2 as having a constant pumping rate, and adjusting q_i and potentially also C_i. Since the dispersion coefficient is generally thought to be velocity dependent, it can be larger for Test 2 than for Test 1. As for Test 1, the $t = 0$ profile is used as the initial condition for the Test 2 model. Any changes in C_i made for Test 2 need to be made for Test 1 as well, so the Test 1 feed-point strengths may need to be re-adjusted.

Finally, the FFEC profiles obtained during artesian logging are fit using the same z_i and C_i as for Test 1 and Test 2, but with different q_i. Flow conditions in the wellbore are assumed to be constant from the end of the recirculation period until these logs were collected a few hours later. There is no reliable initial condition to use for this model, as no logging was done at the conclusion of recirculation. However, the final effluent salinity of the recirculation water was about 50-65 mS/m, so this provides a first guess for an initial condition. The portion of the artesian FFEC profiles where no peaks are present may also be used to constrain initial conditions. Figure 6 suggests that initial FEC decreases slightly as depth increases. Because recirculation was performed with a large flow rate and the effluent salinity stabilizes, it appears that the FFEC profiles reach steady state during recirculation. In other words, they are composed of step-rate changes in FEC and not isolated peaks. The simplest initial condition consistent with all the above information is used for the artesian logging model: i.e., a three-level initial

condition with FEC = 25 mS/m for z > 489 m, FEC = 40 mS/m for 489 > *z* > 288 m and FEC = 85 mS/m for *z* < 288 m.

4.2 Results

4.2.1 Direct-Fit Analysis

Figures 7, 8, and 9 compare the modeled FFEC profiles with the field data for the case giving the best overall match to Test 1, Test 2 (first 3 profiles), and artesian logs. If only Test 1 were matched by itself, a better match could be obtained, but certain compromises must be made to simultaneously match profiles from all tests. The need to compromise suggests that the model is missing some aspects of the real world, which in fact we know to be the case (e.g., variable wellbore diameter (Figure 1) and variable pumping rate (Figure 2)). Even so, the Test 1 match is quite good. The sum of the feed-point strengths is 6.2 L/min, which is close to the estimate for flow out of the formation Q_{form} = 6.1 L/min. A dispersion coefficient of 0.004 m^2/s is used.

For Test 2, the peaks for the final two profiles are not included in the match. Elsewhere, the match is adequate, but not as good as the match for Test 1. The sum of the feed-point strengths is 11.1 L/min, which is not too far below the estimated value of Q_{form} = 11.9 L/min. A dispersion coefficient of 0.005 m^2/s is used.

For the artesian logs, the match is more qualitative, as only two FFEC profiles are available, and they were not collected consecutively. The sum of the feed-point strengths is 5.3 L/min, which compares reasonably well with an independent estimate of artesian flow rate of 4.6 L/min, obtained from the water-level data shown in Figure 3 (described in Section 5). A dispersion coefficient of 0.003 m^2/s is used to match the artesian-logging FFEC profiles. The increase in dispersion coefficient (0.003 m^2/s to 0.005 m^2/s) as flow rate increases from artesian conditions to Test 1 to Test 2 is not surprising, as dispersion is commonly found to increase with flow velocity.

Altogether, the matches shown in Figures 7, 8, and 9 are considered good enough to indicate that we are correctly capturing the key features of flow in the fractures

intercepted by the wellbore, with the small discrepancies indicating that there are other minor effects not accounted for by our model. Table 1 and Figure 10 show the feed-point strengths q_i and salinities C_i (in terms of FEC) inferred from the analysis of Test 1, Test 2, and the artesian logging. Note that the deepest peak shows little evidence of upflow. It is hypothesized that this peak represents horizontal flow past the wellbore at this depth. The horizontal flow is represented by pairs of feed points at the same depth (z_i = 487 and 469 m). Within each pair, one feed point represents inflow from the formation to the wellbore and the other feed point represents outflow from the wellbore to the formation. For artesian logging, when flow up the well is smallest, the inflow and outflow feed points have nearly equal strengths, but opposite signs. When pumping occurs, as during Test 1 and Test 2, wellbore pressure is lower, flow up the well is greater, and more inflow and less outflow occurs, as one would expect.

For isolated peaks at 470 m and 360 m, the choice of dispersion coefficient strongly affects peak height, and consequently makes the choice of feed-point salinity C_i uncertain. A smaller dispersion coefficient produces a peak that is higher and narrower; thus C_i must be smaller. For a larger dispersion coefficient, the peak is lower and wider, thus C_i must be larger. (For the interfering peaks in the upper half of the logged zone, the choice of dispersion coefficient has little impact on the profile, making the choice of C_i there relatively more certain.) If only Test 1 and Test 2 are matched simultaneously, salinity of the peak at 470 m can range from 2000 – 5000 mS/m and adequately match the FFEC profiles. However, when the artesian logs are also included, the range of possible salinities greatly decreases, making the 3000 mS/m value chosen much better constrained. In contrast, the salinity of the small peaks at 400 m depth remains very poorly constrained within the range 1500 – 3000 mS/m. The lower value of C_i would double q_i, but the q_i value itself is so small that doubling it would not significantly worsen the match for the shallower part of the profile.

After the direct-fit analysis was completed, three EC measurements made on effluent collected during the late-time period of pumping tests on packed-off intervals were made

available. These are shown in Figure 10. The agreement is quite good, enhancing confidence in the validity of the FFEC analysis results.

4.2.2 Mass-Integral Analysis

Figure 11 shows results of the mass-integral analysis for Test 1 and Test 2 and the artesian logging. The data points show $M(t)$, FEC integrated over the entire logged interval for each FFEC profile. (If FEC were converted to salinity units mg/L, $M(t)$ would represent the mass of salt in the borehole as a function of time). For a constant pumping-rate test with constant feed-point strength and salinity, $M(t)$ would increase linearly from $t = 0$. Figure 11a shows a good fit to a straight line for Test 1, confirming that averaging out the small pumping-rate variations shown in Figure 2 is reasonable. In contrast, Figure 11b shows that for Test 2, $M(t)$ decreases more slowly for the final two profiles, consistent with the significant decrease in pumping rate that occurred just before four hours (Figure 2). The $M(t)$ profiles for both tests show good linearity at early times, suggesting that feed-point salinities C_i are constant in time, which would not be the case if a significant amount of DI water was pushed out into the fractures during recirculation. In fact, the large non-zero values of $M(0)$ indicate that significant amounts of native water flowed into the wellbore under artesian conditions prior to the onset of pumping at $t = 0$. The $M(-1.5)$ values calculated for the artesian FFEC profiles confirm this. Linear interpolations between the $M(t)$ values for the end of recirculation (based on the step initial conditions for the artesian logging) and the $M(0)$ values (obtained by linear fit to the Test 1 and Test 2 $M(t)$ values) are also shown in Figure 11. Note that the slopes of these lines are smaller than the slopes under pumping conditions. If we assume that feed-point salinity C_i does not change in time, the ratios of the slopes of the $M(t)$ lines for artesian and pumping conditions can be used to estimate the artesian flow rate, which was not measured during field operations. Test 1 yields Q = 4.5 L/min and Test 2 yields Q = 4.4 L/min. These values are somewhat smaller than the Q = 5.3 L/min obtained for the artesian flow rate by direct fitting, and examination of that fit (Figure 9) does suggest that the model's overprediction for the interval 180 m < z < 230 m would be ameliorated by using a smaller value of Q.

For Test 1, all model values of $M(t)$ match the data reasonably well, as do the first four values for Test 2, consistent with the good matches to the FFEC profiles themselves shown in Figure 7 and Figure 8. The slight overprediction of the model for the first two times of Test 2 can probably be explained by the non-linear water-level decline for Test 2 (Figure 3): the larger change in water-level for the first hour produces a larger Q_{well}, which in turn produces a smaller Q_{form}, compared to the model, resulting in smaller actual values of $M(t)$ than predicted by the model.

4.2.3 Multi-rate Analysis

Following the joint fitting of Test 1, Test 2, and the artesian profiles, a standard multi-rate analysis (Tsang and Doughty, 2003; Doughty and Tsang, 2005) was done on the results shown in Table 1. This analysis uses Equations (1) and (2) to produce estimates of transmissivity and hydraulic head for each feed point, as shown in Table 2 and Figure 12. Transmissivity for the ith feed point T_i is given in dimensionless form as T_i/T_{tot}, where T_{tot} is the transmissivity of the entire logged interval. Hydraulic head is shown as a normalized group $I\Delta P_i$, where positive values indicate a driving force for flow from the formation into the wellbore under shut-in conditions and negative values indicate a driving force for flow from the shut-in wellbore into the formation. Multi-rate analysis uses q_i values from two tests at a time, and was done twice: once using Test 1 and Test 2 results, and once using Test 1 and artesian-logging results. All the transmissivity results show good agreement between the two analyses, as do most of the hydraulic head results. Where the two analyses give similar results, confidence in the result is higher. The relatively poor agreement for the peaks around 400 m depth is not surprising; uncertainty in feed-point parameters is especially large for these peaks because they are so small that they can be matched with different combinations of parameters. Agreement between the two cases is not so good for the 280-290 m depth either, but peaks here interfere strongly at all times, making analysis less certain. For the deepest portion of the logged interval (470 - 490 m), the positive and negative hydraulic heads required to produce horizontal flow across the borehole are clearly evident.

Table 2 summarizes the main results of multi-rate FFEC logging in borehole PB-V01: feed-point depth, salinity, transmissivity, and hydraulic head for 15 inflow points, and depth, salinity, and local velocity past the borehole for the two deep horizontal flow zones. Local velocity $v_{natural}$ represents flow across the borehole diameter in the fracture plane, but it is not necessarily equal to the regional (average) groundwater velocity through the fractured rock. Drost et al. (1968) have discussed flow focusing for boreholes in porous formations and proposed a simple correction factor, but the situation is more complicated for flow through a network of rock fractures.

Note that obtaining distinct values of hydraulic head for different feed points does not imply that the fractures must be hydrologically isolated from one another. It merely indicates that there is a driving force for flow between them; whether or not flow occurs depends on the connectivity of the fracture network. Conversely, if hydraulic head is the same for multiple feed points over a depth range, it suggests that they probably are in hydrologic communication, but again it does not guarantee that any two fractures are connected.

Once values of T_i/T_{tot} for each feed point have been obtained, it is straightforward to use Equation (2) to assign $q_i(t)$ values corresponding to $Q(t)$ for a variable pumping rate test. This is done for Test 2, assuming $Q(t)$ takes the two-level form of the red line shown in Figure 2. A comparison of model and field FFEC profiles is shown in Figure 13. Despite the decrease in feed-point strength applied just before 4 hours, modeled peak height is too large for profiles for t = 3 hours, t = 4 hours, and t = 5 hours. We hypothesize that something beyond the scope of our conceptual model may have decreased C_i or q_i or both, between t = 2 and t = 3 hours. Another possibility is that a flaw developed in the EC probe that damped out large values of FEC, as the non-peak portions of the FFEC profiles appear reasonable for all times.

5. Comparison with Packer Tests

Figure 12 shows packer-test results for transmissivity and hydraulic head, provided by JAEA after FFEC analysis was completed. Transmissivities were determined by matching pressure data to standard analytical solutions by Hvorslev (1951), Cooper et al. (1967), and Agarwal (1980). As noted in the introduction, packer tests are a well-established, widely-used means of determining fracture transmissivity. However, we do not expect them to produce identical results to FFEC logging because in a packer test, pumping is from one interval at a time, whereas in FFEC logging the entire logged interval is pumped at once. If the fractures intercepting the wellbore form a connected network, they will respond somewhat differently to these different pumping schemes (Doughty et al., 2005).

Because packer intervals may cover more than one fracture (packer-test resolution being much coarser than results from the FFEC logging analysis), it is not possible to make a one-to-one comparison between the FFEC transmissivities and packer-test transmissivities (Figure 12a). However, the FFEC results for individual feed points can be averaged over the depth intervals of the packer tests to allow comparison. To convert the packer-test results for an interval L (transmissivity T_L in m^2/s and hydraulic head P_L in m) into FFEC logging results (groups T_i/T_{tot} and $I\Delta P_i$), we proceed as follows. Of all the packer tests, we select six whose length intervals cover the logged interval of the borehole (shown as black line segments in Figure 12). The sum of the T_L values for these six intervals is then T_{tot}. The basic result is T_L/T_{tot}, but we divide this quantity by n_L, the number of feed points for each interval L, to enable ready visual comparison with individual feed point values T_i/T_{tot}. To convert P_L to $I\Delta P_L$, we first average the six P_L values to form P_{avg}, using $P_{avg} = \Sigma(T_L P_L)/T_{tot}$, where the sum runs over the six packer-test intervals. The value of productivity index I is calculated as the slope of the line plotting flow from the formation versus steady-state drawdown for Tests 1 and 2 (Figure 14). For a non-artesian well, Equation (3) could be used directly to determine I, but here we must use the slope. Drawdown is estimated from the water-level data shown in Figure 3, and

flow rate is taken from the direct-fit values: 6.2 L/min for Test 1 and 11.1 L/min for Test 2 (similar results would be obtained using the Q_{form} values of 6.1 and 11.8). This yields a slope I = 0.27 L/min per m. By extrapolating the line to a drawdown of 0, we obtain an independent estimate for the artesian flow rate of 4.6 L/min. With I and P_{avg} determined, it is straightforward to form $I\Delta P_L = I(P_L - P_{avg})$, which may be compared directly with individual feed point values $I\Delta P_i$.

Generally, the transmissivity values for FFEC logging and packer tests agree within 50%, which we consider pretty good agreement. Note that Figure 12 plots transmissivity on a linear scale, whereas fracture transmissivity can easily vary over several orders of magnitude. The match is especially good for the largest transmissivity fractures, around depths of 235 to 315 m. On the other hand, the hydraulic head values for FFEC logging and packer tests only agree well for the large-transmissivity zone from 250-315 m depth and the moderate-transmissivity zone from 315-380 m depth. With the exception of the small peaks around 400 m depth (whose low transmissivity makes hydraulic head estimation uncertain), the packer tests show a small increase in hydraulic head with depth. While none of the FFEC hydraulic head values grossly differ from the packer-test results, this overall trend is not evident in the FFEC results.

Figure 12 also shows packer-test results for shorter packed-off intervals (green line segments), which were chosen to represent specific features from the fracture log (Figure 1). Comparison to the FFEC-derived transmissivities for individual feed points or groups of 2-3 adjacent feed points is reasonably good, and in fact suggests a productive means of using FFEC logging as part of packer-test design, to identify the optimal locations for packer placement. Hydraulic heads obtained from short-interval packer tests (green segments) are quite consistent with those obtained from long-interval packer tests (black segments), and show much less variability than do the FFEC-determined hydraulic heads.

6. Discussion

The main operational difficulties encountered during the FFEC logging of borehole PB-V01, along with their consequences for analysis, are listed below, in order of increasing severity. (1) Artesian flow rate is unknown (and may not even be constant), thus the feed point strengths q_i inferred from artesian logging cannot be constrained by $\Sigma q_i = Q$. (2) Pumping rate cannot be held constant, precluding the use of all FFEC profiles in the multi-rate analysis. (3) Water-level decline during logging is non-linear, precluding reliable calculation of Q_{well} and hence Q_{forrm}, again eliminating use of the constraint $\Sigma q_i = Q_{form}$. (4) Water-level decline is not simply correlated to changes in pumping rate, possibly invalidating the employed conceptual flow model. Note that these operational difficulties do not preclude the use of artesian wells for FFEC logging, but they point out the value of imposing careful testing control and monitoring.

Nonetheless, despite these complications in the current FFEC logging, the FFEC analysis results are largely consistent, and reasonable. The small non-systematic variations in pumping rate observed in Test 1 apparently can be neglected. For Test 2, the first four hours, with approximately constant rate, can be used for the multi-rate analysis, and then the longer-term variation can be modeled separately. Reasonable values for artesian flow rate are obtained by linearizing water-level declines for Tests 1 and 2.

It is difficult to assign simple, quantitative measures of uncertainty to the parameters inferred from FFEC logging, because of the way unknown parameters combine to create the features observed in the FFEC logs. Under ideal conditions – uniform initial conditions, constant pumping rate and wellbore water level, peaks that do not interfere with one another right away, and logging that lasts until steady state is achieved – feed-point strengths and salinities could be uniquely determined (Tsang et al., 1990), so transmissivity and hydraulic head could be uniquely determined as well (Equations 1 and 2). However, such ideal conditions are rarely encountered in the field, and two problems decreasing the sensitivity to individual parameters are commonly encountered. First, if logging does not last long enough for plateaus to form as peaks are skewed up the wellbore, then the peak height merely depends on the product q_iC_i, making identification of q_i and C_i individually difficult. Second, if peaks interfere during even the earliest log, then identifying parameters of individual peaks becomes difficult. In general, one cannot specify a

minimum feed-point strength or salinity that will produce an identifiable peak – it depends on the location of that peak among all the others. One way to assess the sensitivity of FFEC profiles to feed-point parameters, and consequently the uncertainty of inferred properties, is to do sensitivity studies with BORE II. To this end, various arrangements of feed points and the corresponding FFEC profiles they create have been examined in Doughty and Tsang (2005), to create a catalog of 'signatures' in FFEC logs that illustrate the sensitivity to unknown feed-point parameters.

The comparison with packer test results indicates that the T_i/T_{tot} appear to be determined more reliably than $I\Delta P_i$ for FFEC logging under non-ideal conditions, which was also suggested by a previous study (Doughty et al., 2008). This finding may not be surprising when one considers the form of the equations used to derive these parameters. Equation (1) shows that T_i/T_{tot} depends on the difference between two inferred parameters $q_i^{(1)}$ and $q_i^{(2)}$, making T_i/T_{tot} rather uncertain when one or both q_i values are poorly constrained or are similar in value to one another. In contrast, Equation (2) can be rearranged to show that $I\Delta P_i$ depends on the difference between inferred parameter $q_i^{(1)}$ and already uncertain T_i/T_{tot}, which introduces an extra level of uncertainty.

7. Conclusions

Despite complications arising from the use of an open artesian well for multi-rate FFEC logging, reasonable results can be obtained on feed-point location, strength, salinity, and transmissivity. The inferred salinities agree well with three independently-measured salinity values obtained during pumping tests in selected packed-off intervals. Feed-point transmissivities determined with FFEC logging are generally consistent with those obtained from independent packer tests. Actually, FFEC logging has provided information on fracture transmissivity with far greater spatial resolution than can be achieved with packer tests, and has done so in a much shorter length of time. Because the hydraulic head results from FFEC logging do not consistently reproduce the trend obtained from the packer tests, they are considered to be less reliable, which is not surprising, given the non-ideal operating conditions encountered during FFEC logging and the form of the equations used to derive these hydraulic heads.

The artesian nature of the well is not in itself a problem. If artesian flow rate were measured and found to remain reasonably constant throughout the logging period, there would be no difference from analysis of a pumped well. However, here artesian flow rate was unknown during the artesian logging and pumping rate was not well controlled during pumped logging. Furthermore, it was difficult to develop a consistent conceptual model for the variability of water level with pumping rate during logging.

Despite these complications, results in Table 2 demonstrate the power and usefulness of the multi-rate FFEC logging method. In two tests lasting only about 12 hours each, detailed hydraulic data for 17 fractures intercepted by a borehole are obtained, including natural flow rates in two of them. The strong variation in hydraulic characteristics among these fractures is to be expected in fracture rocks, which are commonly modeled by discrete fracture network (DFN) models. Data such as those shown in Table 2 will be important information to validate or constrain the construction of DFN models.

Based on the analysis of the multi-rate FFEC logging for borehole PB-V01 at Horonobe, Japan, the following recommendations for future applications of FFEC logging to artesian wells can be made:

1) When FFEC logging is done in an artesian well, it would be beneficial to employ a packer at the top of the well or the top of the logged interval, to help control the flow rate out of the logged section. If this is not practical, at least the artesian flow rate should be monitored.
2) When doing artesian logging, collecting a series of FFEC profiles at regularly spaced tine intervals would greatly improve the analysis of the profiles. The first FFEC profile should be collected as soon as possible after the end of the recirculation period.
3) Water-level data should be measured carefully during logging as it is important for estimating Q_{well} and Q_{form} to provide a constraint on the sum of the feed-point flow rates, to determine productivity index I, and to provide consistency checks on the conceptual model for flow rate and drawdown.

Acknowledgements

We are grateful to Keisuke Maekawa and Atsushi Sawada of Japanese Atomic Energy Agency (JAEA) for helpful discussion, and to Kenzi Karasaki of Lawrence Berkeley National Laboratory (LBNL) and the Journal editor and three anonymous reviewers for careful reviews of the manuscript. This work was supported by the JAEA under the Bi-national Research Cooperation Program between JAEA and the U.S. Department of Energy, Office of Civilian Radioactive Waste Management, Office of Science and Technology. This paper was prepared while the second author (Tsang) was a Visiting Professor at Department of Earth Sciences and Engineering, Imperial College London, whose hospitality is very much appreciated. The work was performed under the auspices of the U.S. Department of Energy through contract to LBNL, Contract No. DE-AC02-05CH11231.

References

Agarwal, R.G., 1980. A new method to account for producing time effects when drawdown type curves are used to analyze pressure buildup and other test data. SPE-9289, presented at the 55th SPE Annual Technical Conference and Exhibition, Dallas, Tex., 21–24 Sept.

Almen, K.E., Editor, 1994. Aspo Hard Rock Laboratory: Feasibility and usefulness of site investigation methods: Experience from the pre-investigation phase. Rep. TR-94-74, Swedish Nuclear Fuel and Waste Management Co. (SKB), Stockholm.

Bauer, G.D. and J.J. LoCoco, 1996. Hydrogeophysics determines aquifer characteristics. International Ground Water Technology 12-16, August/September.

Bear, J., C.-F. Tsang, G. de Marsily, Editors,1993. Flow and contaminant transport in fractured rock, Academic Press, San Diego.

Brainerd, R.J. and G.A. Robbins, 2004. A tracer dilution method for fracture characterization in bedrock wells. Ground Water 42(5), 774-780.

Brauchler, R., R. Liedl, P. Dietrich, 2003. A travel time based hydraulic tomographical approach, Water Resources Res., 39(12), 1370, doi:10.1029/2003WR002262.

Cooper, H.H., J.D. Bredehoeft, and S.S. Papadopulos, 1967. Response of a finite-diameter well to an instantaneous charge of water. Water Resources Res., 3(1), 263–269, doi:10.1029/WR003i001p00263.

Doughty, C. and C.-F. Tsang, 2000. BORE II – A code to compute dynamic wellbore electrical conductivity logs with multiple inflow/outflow points including the effects of horizontal flow across the well. Rep. LBL-46833, Lawrence Berkeley National Laboratory, Berkeley, CA.

Doughty, C. and C.-F. Tsang, 2005. Signatures in flowing fluid electric conductivity logs. J. of Hydrology 310, 157-180.

Doughty, C., S. Takeuchi, K. Amano, M. Shimo and C.-F. Tsang, 2005. Application of Multi-rate Flowing Fluid Electric Conductivity Logging Method to Well DH-2, Tono Site, Japan. Water Resources Res. 41, W10401, doi:10.1029/2004WR003708.

Doughty, C., C.-F. Tsang. K. Hatanaka, S. Yabuuchi and H. Kurikami, 2008. Application of direct-fitting, mass-integral, and multi-rate methods to analysis of flowing fluid electric conductivity logs from Horonobe, Japan. Water Resources Res. 44, W08403, doi:10.1029/2007WR006441.

Drost, W., D. Klotz, A. Koch, H. Moser, F. Neumaier, and W. Rauert, 1968. Point dilution methods of investigating ground water flow by means of radioisotopes. Water Resources Res. 4(1), 125-146.

Enachescu, C.and N. Rahm, 2007. Method evaluation of single hole hydraulic injection tests at site investigations, Oskarshamn Site Investigation. Report P-07-94, Swedish Nuclear Fuel and Waste Management Co. (SKB), Stockholm

Evans, D.G., 1995. Inverting fluid conductivity logs for fracture inflow parameters. Water Resources Res. 31(12), 2905-2915.

Evans, D.G., W.P. Anderson, Jr., and C.-F. Tsang, 1992. Borehole fluid experiments near salt contamination sites in Maine. In proceedings of the NGWA Conference on Eastern Regional Ground Water Issues, Boston, 797-807.

Guyonnet, D., A. Rivera, S. Löw and N. Correa, 1993. Analysis and synthesis of fluid logging data from Wellenberg boreholes SB1, SB3, SB4 and SB6. Nagra Tech. Rep. NTB 92-01, pp. 153, Nagra, Wettington, Switzerland.

Hale, F.V. and C.-F. Tsang, 1988. A code to compute borehole conductivity profiles from multiple feed points. Rep. LBL-24928, Lawrence Berkeley Laboratory, Berkeley, CA.

Hama, K., T. Kunimaru, R. Metcalfe, and A.J. Martin, 2007. The hydrogeochemistry of argillaceous rock formations at the Horonobe URL site, Japan. Phys. Chem. Earth, Parts A, B, and C 32(1-7), 170-180.

Hvorslev, M.J., 1951. Time lag and soil permeability in ground-water observations. Bull. 36, pp. 1– 50, Waterways Exp. Stn., U.S. Army Corps of Eng., Vicksburg, Miss.

Illman, W.A., X. Liu, S. Takeeuchi, T.J. Yeh, K. Ando, and H. Saegusa, 2009. Hydraulic tomography in fractured granite: Mizunami Underground Research site, Japan. Water Resour. Res., 45, WO1406, doi:10.1029/2007WR006715.

Karasaki, K., B. Freifeld, A. Cohen, K. Grossenbacher, P. Cook, and D. Vasco, 2000. A multidisciplinary fractured rock characterization study at Raymond field site, Raymond, CA. J. of Hydrology, 236, 17-34.

Kelley, V. A., J. M. Lavanchy, and S. Löw, 1991. Transmissivities and heads derived from detailed analysis of Siblingen 1989 fluid logging data. Nagra Tech. Rep. NTB 90-09, pp. 184, Nagra, Wettington, Switzerland.

Keys, W.S., 1979. Borehole geophysics in igneous and metamorphic rocks. 20th Annual Logging Symposium Transactions, 1-26, Society of Professional Well Log Analysts, Houston, Tex.

Kowalsky, M.B., E. Gasperikova, S. Finsterle, D. Watson, G. Baker, and S.S. Hubbard, 2011. Coupled modeling of hydrogeochemical and electrical resistivity data for

exploring the impact of recharge on subsurface contamination, Water Resources Res., 47, W02509, doi:10.1029/2009WR008947.

Löw, S., V. Kelley, and S. Vomvoris, 1994. Hydraulic borehole characterization through the application of moment methods to fluid conductivity logs. J. App. Geophys. 31(1-4), 117-131.

Marschall, P. and S. Vomvoris (editors), 1995. Grimsel Test Site: Developments in hydrotesting, fluid logging and combined salt/heat tracer experiments in the BK Site (Phase III). Nagra Tech. Rep. 93-47, Nagra, Wettingen, Switzerland.

Molz, F.J., R.H. Morin, A.E. Hess, J.G. Melville, and O. Guven, 1989. The impeller meter for measuring aquifer permeability variations: evaluation and comparison with other tests. Water Resources Res. 25(7), 1677-1683.

National Research Council, 1996. Rock fractures and fluid flow: contemporary understanding and applications, National Academy Press, Washington, D.C.

Öhberg, A. and P. Rouhiainen, 2000. Groundwater flow measuring techniques. Posiva 2000-12, Posiva Oy, Helsinki, Finland.

Paillet, F.L., 1991. Use of geophysical well logs in evaluating crystalline rocks for siting of radioactive waste repositories. The Log Analyst, 33(2), 85-107.

Paillet, F.L., 1998. Flow modeling and permeability estimation using borehole flow logs in heterogeneous fractured formations. Water Resources Res. 34(5), 997-1010.

Paillet, F.L. and W.H. Pedler, 1996. Integrated borehole logging methods for wellhead protection applications. Engineering Geology 42(2-3), 155-165.

Pedler, W.H., C.L. Head, and L.L. Williams, 1992. Hydrophysical logging: A new wellbore technology for hydrogeologic and contaminant characterization of aquifers. National Outdoor Action Conference, National Ground Water Association, Las Vegas, Nevada.

Rhen I., and L. Hartley, 2009. Bedrock hydrogeology Laxemar, Site descriptive modeling. Rep. R-08-92 (Table 4.1), Swedish Nuclear Fuel and Waste Management Co. (SKB), Stockholm.

Rubin, Y. and S.S Hubbard, Editors, 2005. Hydrogeophysics, Water Science and Technology Library, Vol. 50, Springer, The Netherlands, 523 pp..

Schlumberger, Ltd., 1984. Log interpretation charts. New York.

Tsang, C.-F. and C. Doughty, 2003. Multi-Rate Flowing Fluid Electric Conductivity Method. Water Resources Res. 39(12), 1354-1362.

Tsang, C.-F., P. Hufschmied, and F.V. Hale, 1990. Determination of fracture inflow parameters with a borehole fluid conductivity logging method. Water Resources Res. 26(4), 561-578.

Vereecken, H., A. Binley, G. Cassiani, A. Revil, K. Titov, Editors, 2006. Applied Hydrogeophysics, *NATO Science Series, IV*, 71, 383 pp.

Tables

Table 1. Feed-point strengths and salinities inferred from analysis of Test 1, Test 2, and artesian logging.

Peak Number	Depth (m)	q_i for Artesian Logging (L/min)	q_i for Test 1 (L/min)	q_i for Test 2 (L/min)	C_i (mS/m)
1[a]	487	0.037	0.039	0.050	3000
2[a]		-0.035	-0.030	0.000	
3[a]	469.2	0.430	0.460	0.650	3000
4[a]		-0.350	-0.310	-0.150	
5	408	0.005	0.011	0.025	3000
6	398.5	0.007	0.013	0.035	3000
7	362.7	0.430	0.500	0.900	1500
8	357.5	0.260	0.280	0.400	1500
9	331.2	0.060	0.065	0.090	1200
10	322.3	0.250	0.290	0.500	1000
11	288	0.355	0.390	0.650	1200
12	284.6	0.085	0.100	0.200	1200
13	278	1.380	1.470	2.000	900
14	273.8	0.555	0.590	0.800	770
15	265.6	0.490	0.600	1.200	770
16	258	0.060	0.180	0.900	770
17	253.8	0.605	0.730	1.400	770
18	235.9	0.630	0.700	1.100	770
19	214	0.080	0.120	0.350	770

[a]Inflow/outflow pairs that represent horizontal flow past the borehole under shut-in conditions.

Table 2. Feed-point transmissivities T_i/T_{tot} and hydraulic head $I\Delta P_i$ inferred from analysis of Test 1 and Test 2. For the deep horizontal-flow zones, local velocity past the wellbore $v_{natural}$ is given instead of $I\Delta P_i$.

Peak Number	Depth (m)	$v_{natural}$ (m/day)	T_i/T_{tot}	$I\Delta P_i$ (L/min)	C_i (mS/m)
1/2[a]	487	0.3[a]	0.004		3000
3/4[a]	469.2	3.2[a]	0.036		3000
5	408		0.003	-2.3	3000
6	398.5		0.004	-3.3	3000
7	362.7		0.080	-0.1	1500
8	357.5		0.024	5.2	1500
9	331.2		0.005	6.5	1200
10	322.3		0.043	0.6	1000
11	288		0.053	1.2	1200
12	284.6		0.020	-1.3	1200
13	278		0.108	7.4	900
14	273.8		0.043	7.6	770
15	265.6		0.122	-1.3	770
16	258		0.147	-5.0	770
17	253.8		0.137	-0.9	770
18	235.9		0.082	2.4	770
19	214		0.047	-3.6	770

[a]Inflow/outflow pairs that represent horizontal flow past the borehole ; $v_{natural}$ represents the local velocity across the borehole diameter in the fracture plane. To obtain the natural velocity in the fracture itself a correction is needed (cf. Drost et al., 1968)

List of Figures

Figure 1. Caliper log, depth-averaged caliper log, feed-point depths inferred from FFEC logs (flowing fractures), and fracture log from core analysis (all fractures).

Figure 2. Pumping rate (blue line) for Test 1 and Test 2. The black dashed line is the time-averaged pumping rate used for the BORE II models. For Test 2, the two-step pumping rate shown in red was also used for the model, after the multi-rate analysis had been completed. The colored boxes show the times of FFEC logging.

Figure 3. Water-level data during Test 1 and Test 2. The colored boxes show the times of FFEC logging.

Figure 4. FFEC profiles for Test 1, with average pumping rate 6.7 L/min.

Figure 5. FFEC profiles for Test 2, with average pumping rate 14.3 L/min.

Figure 6. FFEC profiles for artesian logging, when the well was not actively pumped.

Figure 7. Modeled and field FFEC data for Test 1.

Figure 8. Modeled and field FFEC data for Test 2, assuming a constant pumping rate.

Figure 9. Modeled and field FFEC data for artesian logging.

Figure 10. (a) Feed-point strengths for Test 1, Test 2, and artesian logging. (b) feed-point salinities (measured in FEC units). The red line segments show EC values measured independently from late-time effluent collected during pumping from packed-off intervals.

Figure 11. $M(t)$ profiles for (a) Test 1 and (b) Test 2, providing an integral of the FFEC profiles over the entire logged interval. $M(t)$ values for the artesian logging conducted prior to each test are also shown.

Figure 12. Multi-rate FFEC analysis results. (a) T_i/T_{tot}, fraction of total transmissivity of logged interval for each feed point. (b) $I\Delta P_i$, normalized hydraulic head for each feed point. Long-interval packer-test results are shown as horizontal black line segments, and horizontal red line segments show FFEC results averaged over packer-test intervals. Short-interval packer-test results are shown as horizontal green line segments

Figure 13. Modeled and field FFEC data for Test 2, assuming a two-level pumping rate.

Figure 14. Flow from the formation and estimated drawdown for Tests 1 and 2, with the slope used to determine productivity index I, and the intercept used to estimate artesian flow rate.

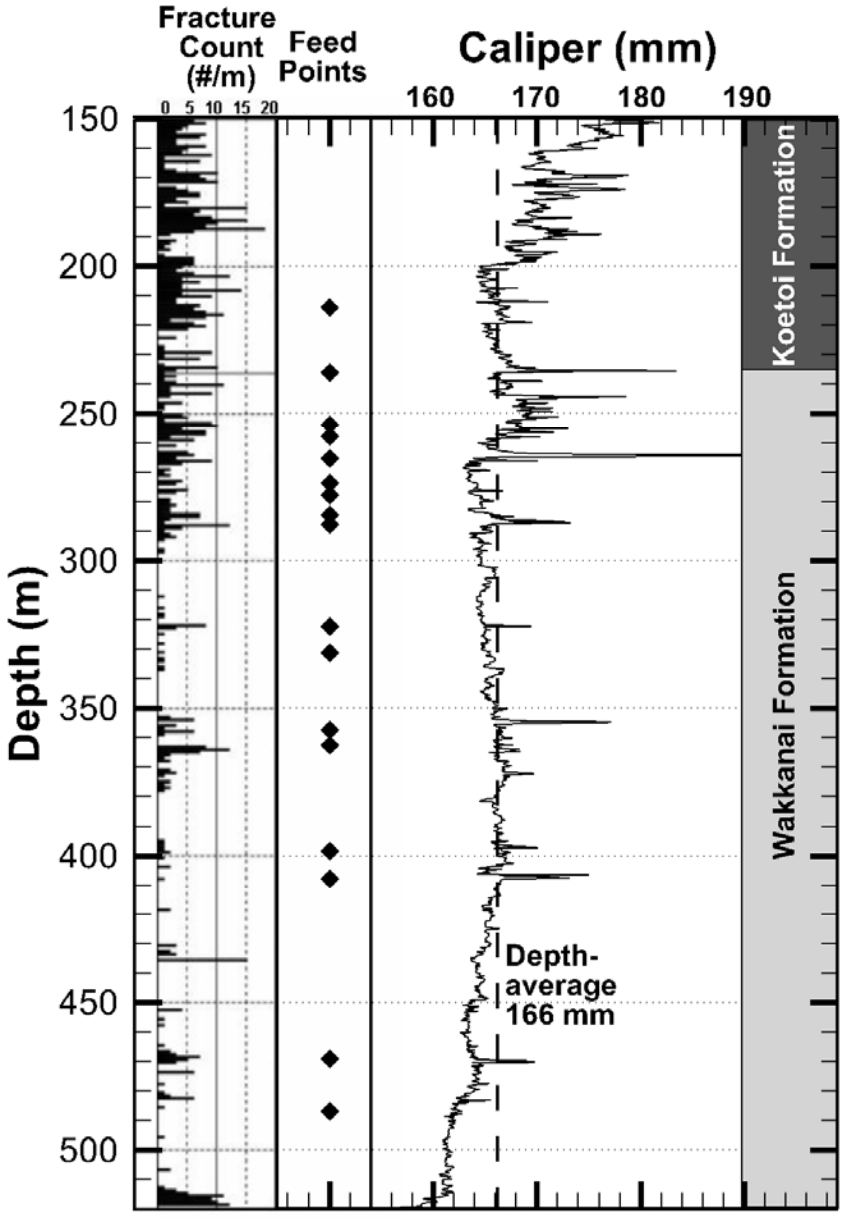

Figure 1. Caliper log, depth-averaged caliper log, feed-point depths inferred from FFEC logs (flowing fractures), and fracture log from core analysis (all fractures).

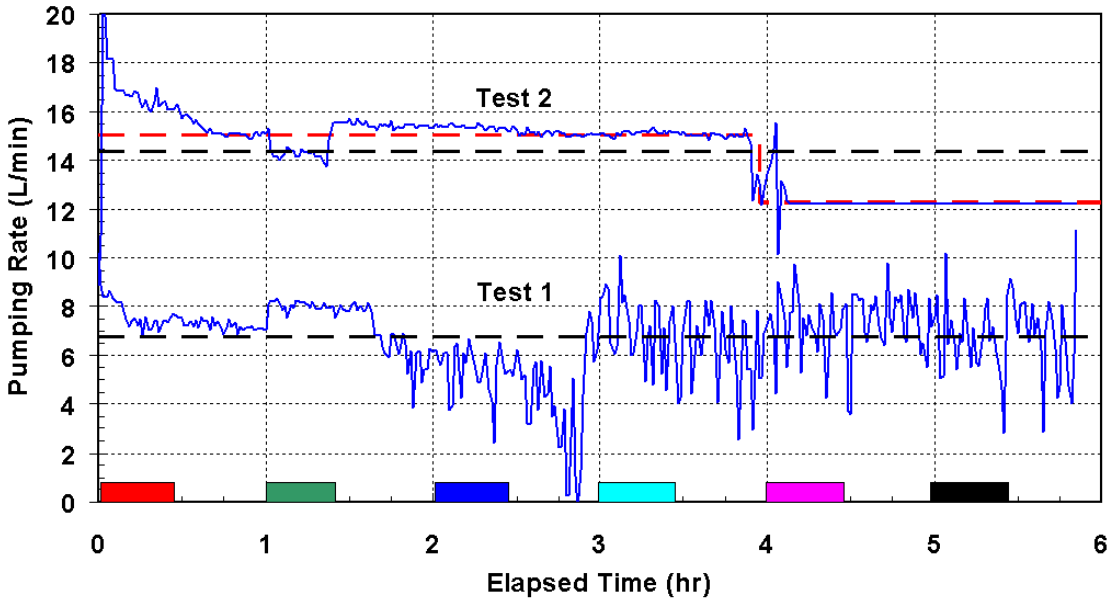

Figure 2. Pumping rate (blue line) for Test 1 and Test 2. The black dashed line is the time-averaged pumping rate used for the BORE II models. For Test 2, the two-step pumping rate shown in red was also used for the model, after the multi-rate analysis had been completed. The colored boxes show the times of FFEC logging.

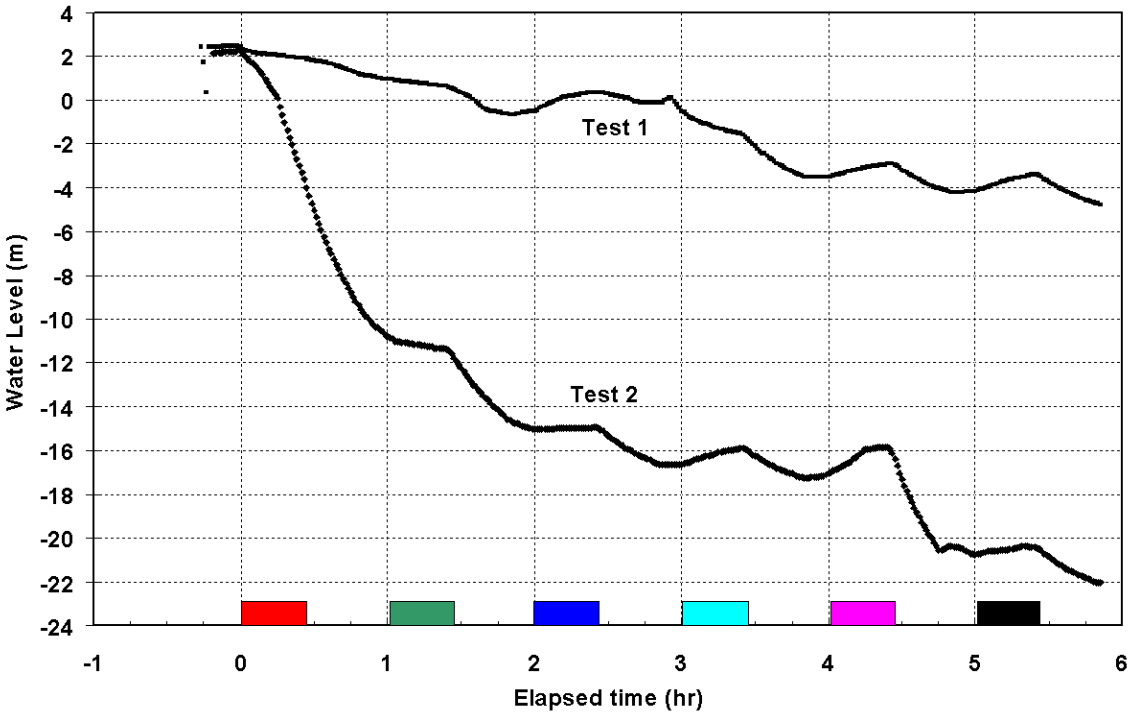

Figure 3. Water-level data during Test 1 and Test 2. The colored boxes show the times of FFEC logging.

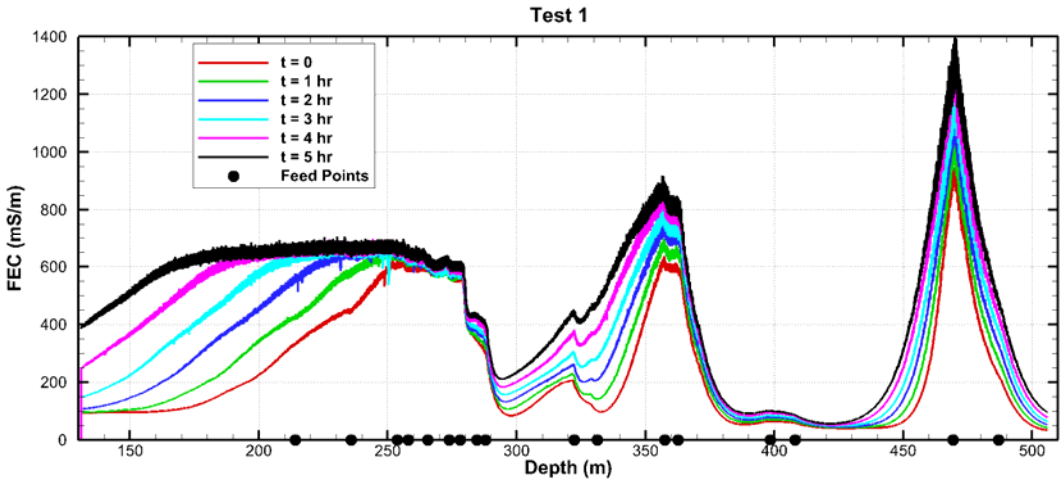

Figure 4. FFEC profiles for Test 1, with average pumping rate 6.7 L/min.

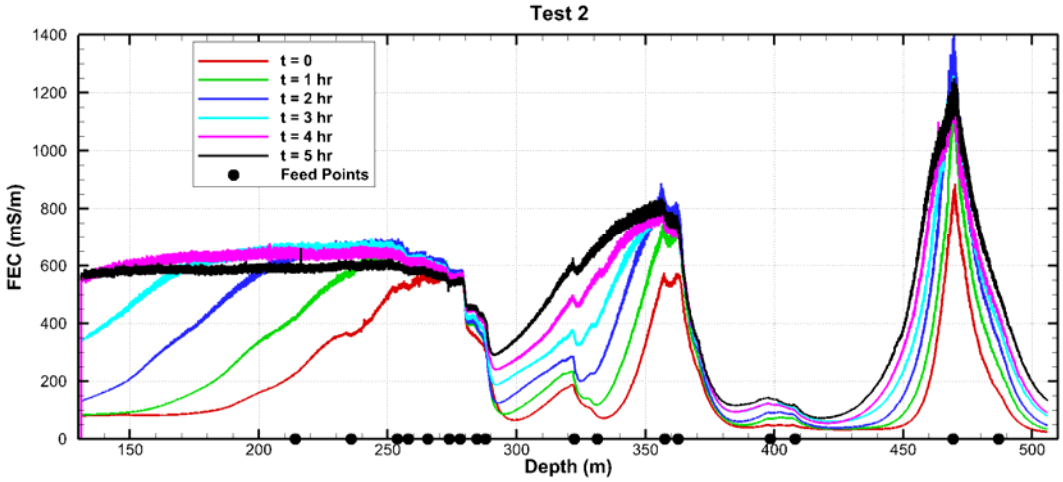

Figure 5. FFEC profiles for Test 2, with average pumping rate 14.3 L/min.

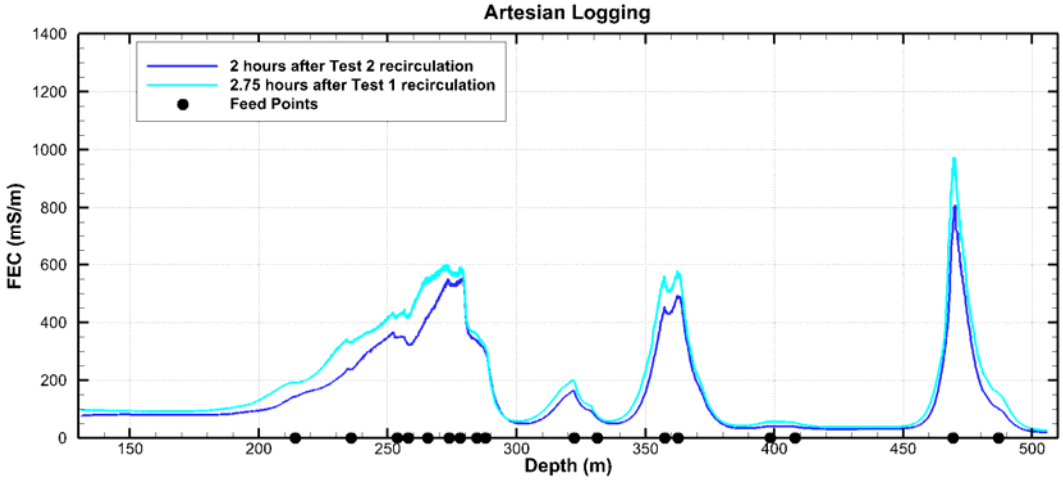

Figure 6. FFEC profiles for artesian logging, when the well was not actively pumped.

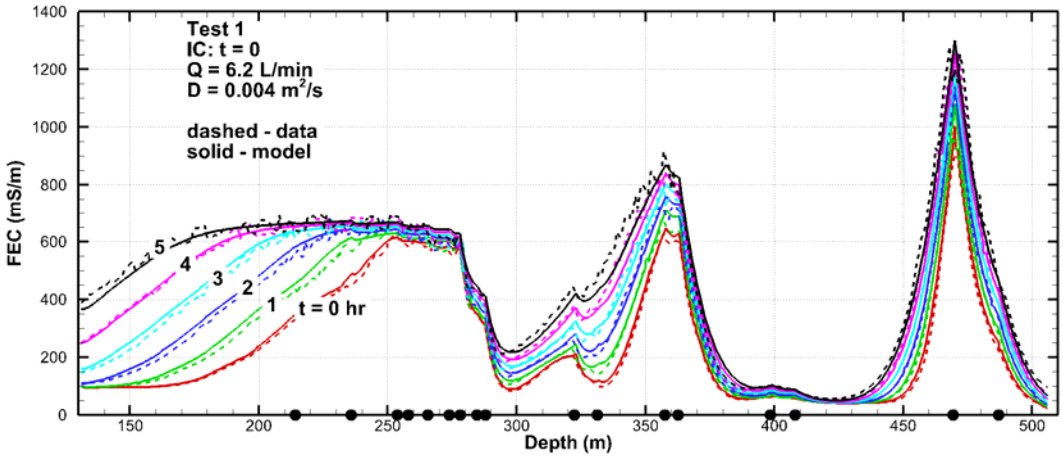

Figure 7. Modeled and field FFEC data for Test 1.

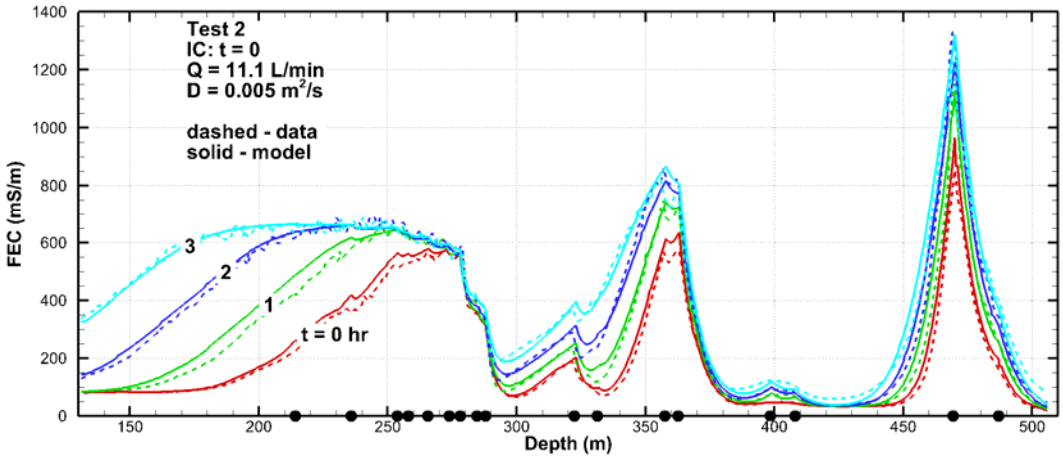

Figure 8. Modeled and field FFEC data for Test 2, assuming a constant pumping rate.

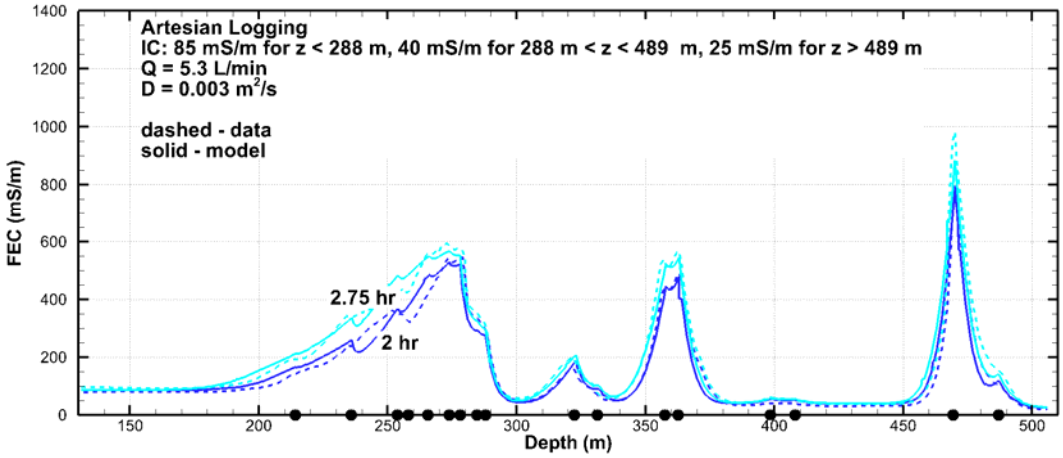

Figure 9. Modeled and field FFEC data for artesian logging.

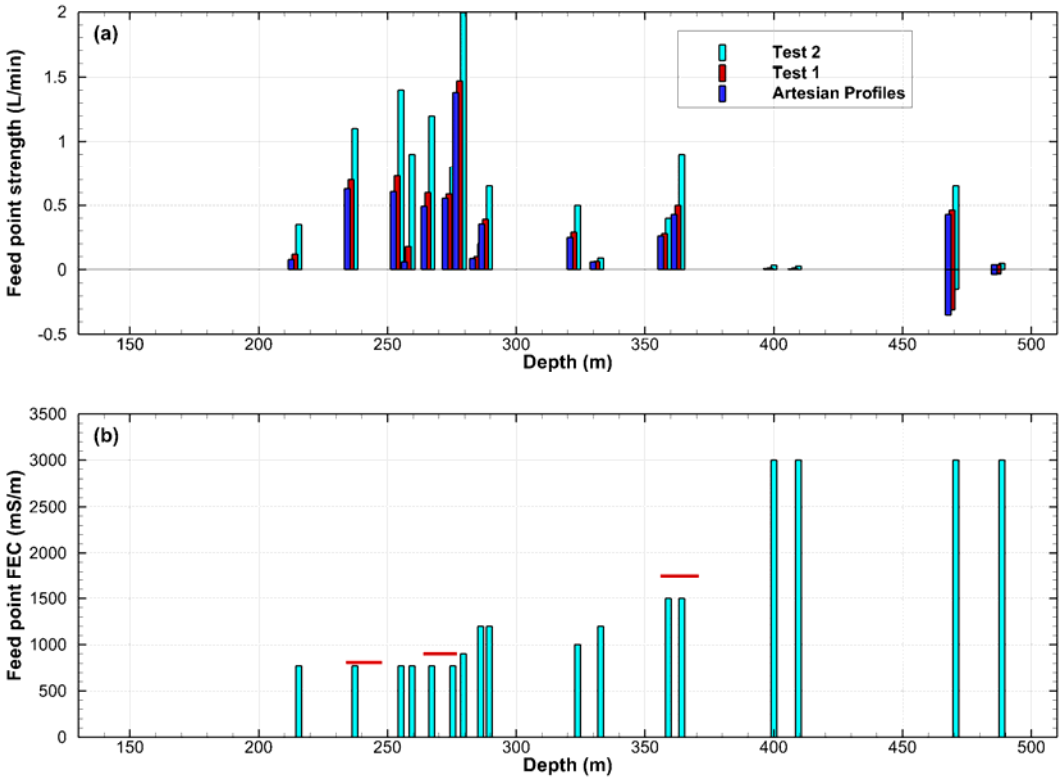

Figure 10. (a) Feed-point strengths for Test 1, Test 2, and artesian logging. (b) feed-point salinities (measured in FEC units). The red line segments show EC values measured independently from late-time effluent collected during pumping from packed-off intervals.

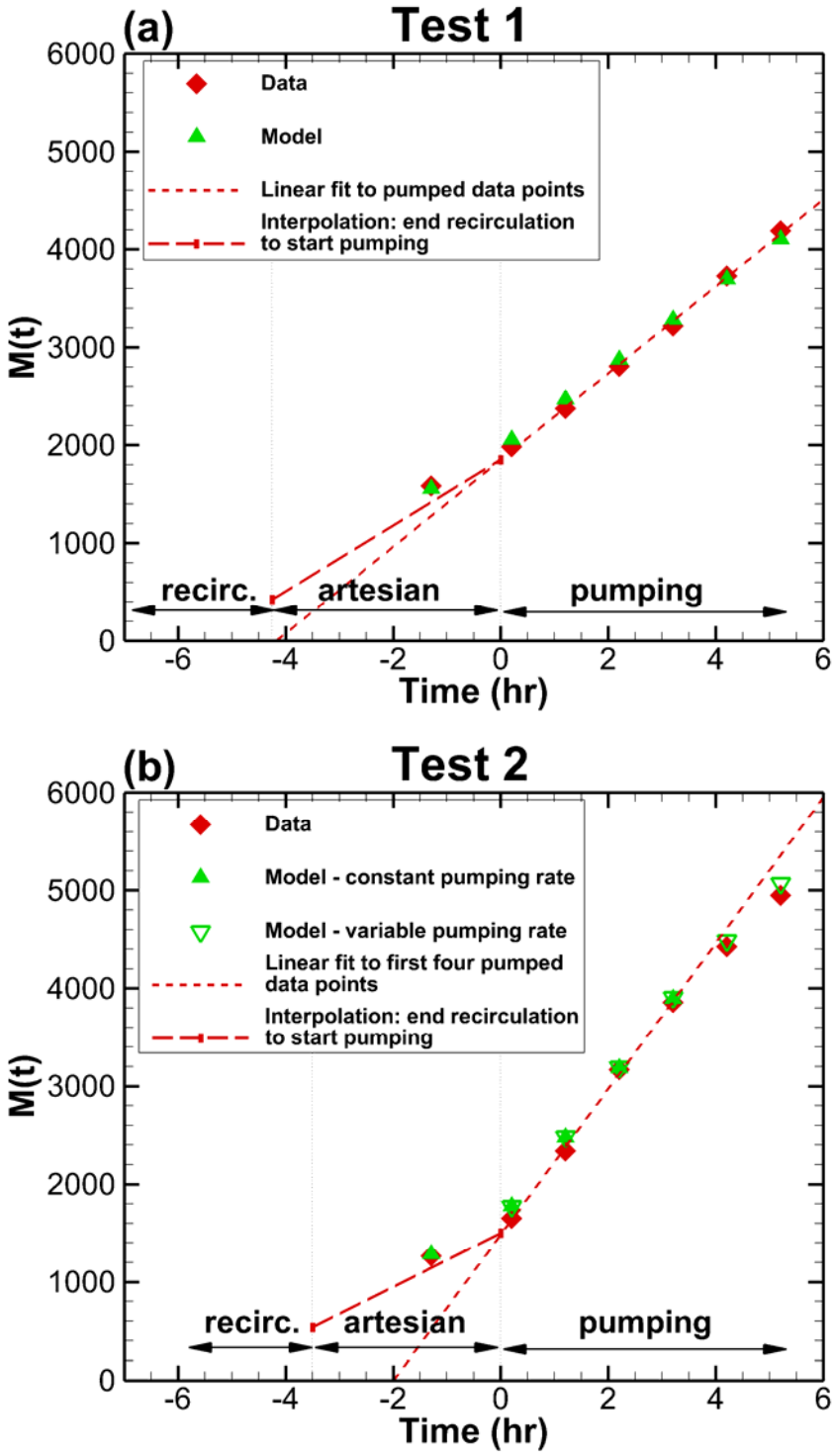

Figure 11. $M(t)$ profiles for (a) Test 1 and (b) Test 2, providing an integral of the FFEC profiles over the entire logged interval. $M(t)$ values for the artesian logging conducted prior to each test are also shown.

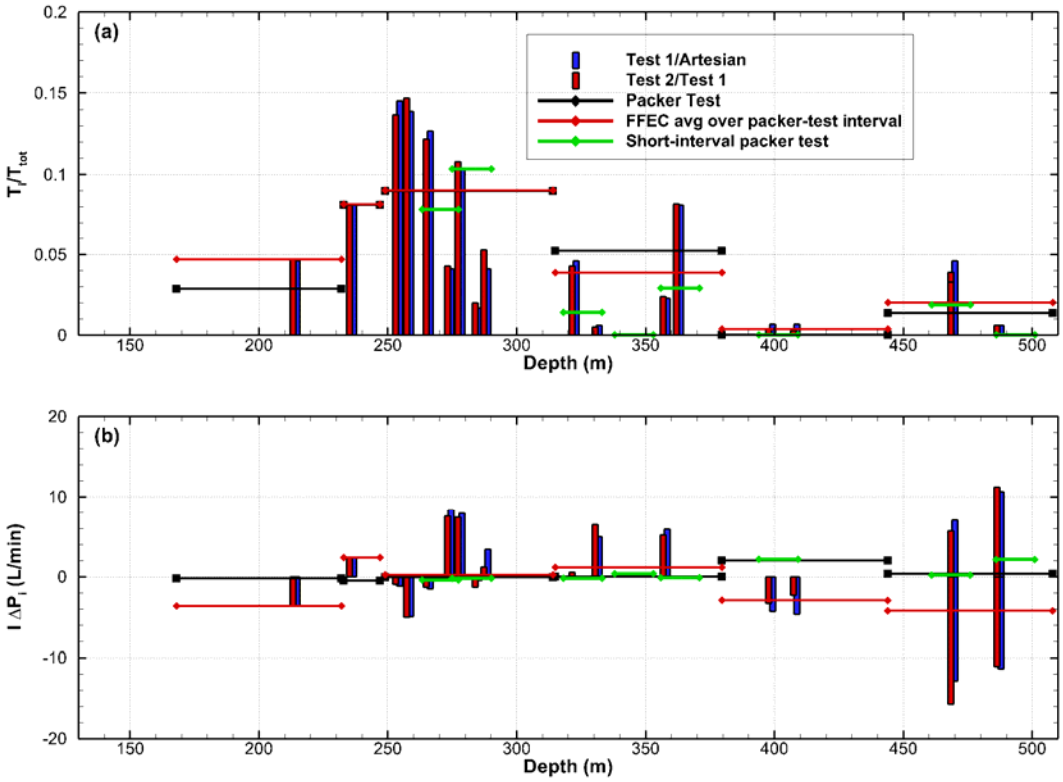

Figure 12. Multi-rate FFEC analysis results. (a) T_i/T_{tot}, fraction of total transmissivity of logged interval for each feed point. (b) $I\Delta P_i$, normalized hydraulic head for each feed point. Long-interval packer-test results are shown as horizontal black line segments, and horizontal red line segments show FFEC results averaged over packer-test intervals. Short-interval packer-test results are shown as horizontal green line segments

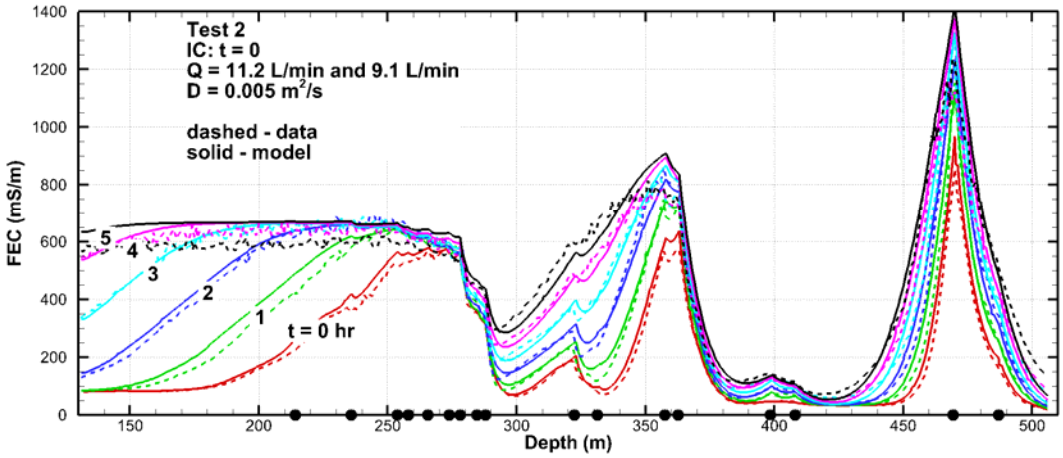

Figure 13. Modeled and field FFEC data for Test 2, assuming a two-level pumping rate.

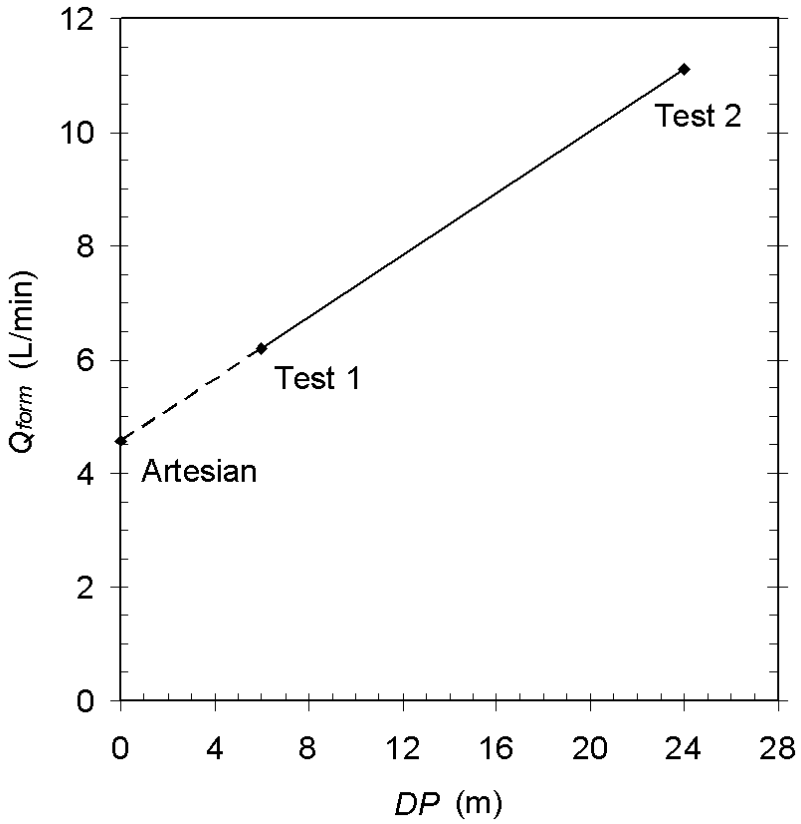

Figure 14. Flow from the formation and estimated drawdown for Tests 1 and 2, with the slope used to determine productivity index *I*, and the intercept used to estimate artesian flow rate.